HVPE epitaxy of semipolar AlN(10$\bar{1}$1) layers on the AlN/Si(100) template

© V.N. Bessolov[1], E.V. Konenkova[1], T.A. Orlova[1], L.A. Sokura[1,2], A.V. Solomnikova[3], Sh.Sh. Sharofidinov[1], M.P. Shcheglov[1]

[1] Ioffe Institute,
194021 St. Petersburg, Russia
[2] ITMO University,
197101 St. Petersburg, Russia
[3] St. Petersburg State Electrotechnical University „LETI",
197376 St. Petersburg, Russia

E-mail: sokuraliliy@mail.ru

Received April 26, 2024
Revised August 28, 2024
Accepted October 30, 2024

The morphology of semipolar AlN(10$\bar{1}$1) layers grown by HVPE on an AlN/Si(100) template with a thickness of 20 nm formed by MOCVD on a nanostructured silicon substrate was studied by AFM method. The average roughness value for semipolar AlN(10$\bar{1}$1) layers was 36 nm for layers with a thickness of 5 mkm, with an *FWHM* (ω-geometry) of about 2.5°. It is shown that such a combined approach of AlN epitaxy on a nanostructured Si(100) substrate results in smoother epitaxial layers.

Keywords: aluminum nitride, nanostructured silicon substrate, vapour-phase epitaxy.

DOI: 10.61011/SC.2024.09.59912.6418A

AlN with a wurtzite structure is a wide-band gap semiconductor with a direct band gap of 6.2 eV, high thermal conductivity [1] and high piezoelectric constant, and therefore is a promising material for the manufacture of ultraviolet optoelectronic devices [2] and high-power high-frequency electronics devices [3]. Thin layers of AlN are widely used as buffer layers for growing of GaN [4]. Due to the limited size and high cost of bulk substrates, AlN layers are typically grown heteroepitaxially on foreign substrates such as sapphire and silicon [5,6].

A significant number of scientific papers are devoted to the study of the properties of wide-band gap polar III-nitride films [7]. One of the fundamental problems hindering the manufacture of devices based on InGaN/GaN and AlGaN/GaN heterostructures is the polar orientation of GaN, which leads to the appearance of piezoelectric fields induced by film deformation resulting from mismatch of lattice parameters at the heterogeneous interface of the semiconductor structure. The InGaN/GaN-based emitters demonstrate a small overlap between the electron and hole wave functions, which leads to a long radiation recombination time and, consequently, low quantum efficiency (the so-called Stark effect). This becomes a problem for both green and mostly for yellow emitters, in which a higher concentration of In is required in the active InGaN layer, and thus the increased deformation creates even stronger piezoelectric fields [7]. It was found that the differences in polarization values at the interface between GaN and InGaN depend on the angle between the semipolar plane and the (0001) plane [8]. Theoretical calculations are presented in Ref. [9], illustrating that the total piezoelectric polarization in $In_xGa_{1-x}N$ semipolar films is significantly lower than the total polarization in such films, but with a polar orientation. On the other hand, it was shown by Smirnov et al. [10] that mechanical stress relaxation is possible in heterostructures of $In_{0.06}Ga_{0.94}N$/GaN with a growth plane (10$\bar{1}$1) due to the formation of mismatch dislocations as a result of both basal and prismatic slip compared with other orientations of the heterostructure. Semipolar AlN(10$\bar{1}$1) layers grown by hydride vapor phase epitaxy (HVPE) on a nanostructured Si(100) substrate demonstrated plastic relaxation of the semipolar layer in the form of parallel dislocation lines, in contrast to plastic relaxation of polar AlN/Si(111) structures, which manifest themselves as a network of mismatch dislocations [11].

Due to the large difference in lattice parameters and thermal expansion coefficients between AlN and Si, the thickness of the AlN layer was limited to $\sim 1\,\mu$m to prevent cracking [12], but this layer thickness is not sufficient to reduce the density of dislocations occurring at the AlN/Si interface [13].

It was reported in Ref. [14] that the use of structured Si(111) substrates made it possible to obtain an AlN layer with a thickness of $8\,\mu$m, and the full width at half maximum (*FWHM*) of the X-ray rocking curves for AlN(10$\bar{1}$2) planes of the resulting layer reached 800 arc. sec. [15].

The purpose of this work is to determine the optimal conditions for the epitaxial growth of semipolar AlN(10$\bar{1}$1) layers grown by the HVPE method both on a nanostructured substrate NP-Si(100) and on an AlN/NP-Si(100) template. To achieve this goal a V-shaped nanostructure NP-Si(100) was produced on the Si(100) substrate by analogy with paper [16], such nanostructure had „ridges" with a period between them of 70 nm and a height of „ridge" of 30–50 nm. NP-Si(100) substrate has faces that

FWHM of X-ray diffraction ω_θ, rms, average roughness value ra for semi-polar AlN layers$(10\bar{1}1)$ grown by HVPE method on different templates

Structure	Orientation of AlN layer	ω_θ, arcgrad	rms, nm	ra, nm
AlN/AlN(MOCVD)/NP-Si(100)	AlN$(10\bar{1}1)$	2.5	49.156	36.956
AlN/NP-Si(100)	AlN$(10\bar{1}1)$/(0001)	3.5	123.098	96.787

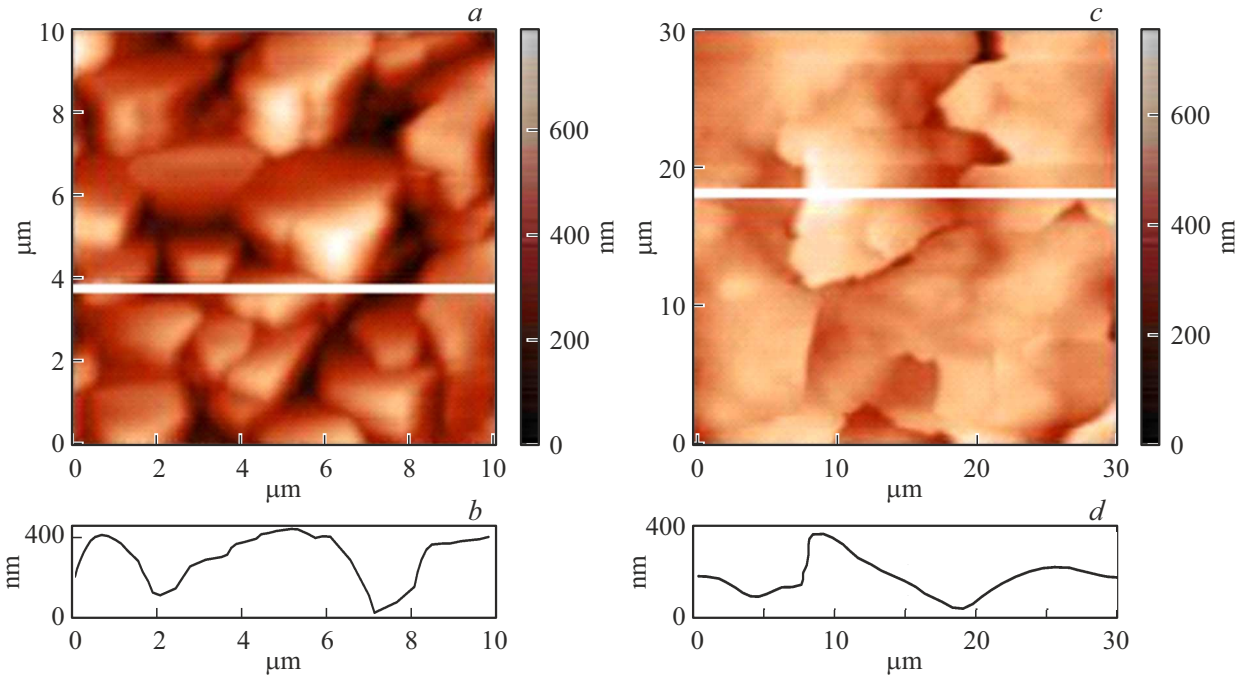

Figure 1. AFM image (a) and profile (b) of the surface of the AlN/NP-Si(100) structure along the growth direction of the semipolar blocks; AFM image (c) and profile (d) the surfaces of the AlN/AlN(MOCVD)/NP-Si(100) structure along the growth direction of the semipolar blocks.

correspond to the plane with angles of tilt $\sim 54°$ — Si(111) faces. The nanostructured substrates were cleaned in a standard way and etched in a solution of hydrofluoric acid with water in a ratio of 1 : 5 for 1 minute, and then buffer layers of AlN with a thickness of 20 nm were grown on the surface by metalorganic vapor phase epitaxy (MOCVD) in a hydrogen atmosphere using a system with a horizontal flow reactor and inductive heating at a temperature of 1080° C. Thick ($\sim 5\,\mu$m) layers of AlN$(10\bar{1}1)$ were epitaxially grown by the HVPE method at a temperature of 1080°C in an argon atmosphere. The growth rates of AlN layers in the MOCVD and HVPE methods were 30 nm/min and 0.6 μm/min, respectively. Growing AlN layers first by the MOCVD method, followed by cooling from the growth temperature to room temperature and further growth of AlN by the HVPE method should lead to a decrease in stresses arising from differences in the coefficients of thermal expansion of the AIN layer and the Si substrate due to stress relaxation in the buffer layer AlN.

The X-ray diffraction patterns of the AlN layers were analyzed using a three-crystal X-ray spectrometer. Rocking curves were received for (0002) and $(10\bar{1}1)$ Bragg reflections in the mode of a two-crystal ω-scan scheme of diffraction.

The study of AlN layers grown on a substrate and template by X-ray diffraction analysis and atomic force microscopy (AFM) showed that the layers have a semipolar block structure $(10\bar{1}1)$, while *FWHM* of X-ray diffraction ω_θ, rms value and average the roughness value ra (square and arithmetic deviation of the profile, respectively) for semipolar layers of AlN$(10\bar{1}1)$ has a significantly lower value in case of an epitaxy of the layer on the AlN(MOCVD)/NP-Si(100) template than on NP-Si(100) substrate (see the Table). Crystallites with two distinct growth planes $(10\bar{1}1)$ and (0001) are formed directly on NP-Si(100) substrate during the growth of the AlN film, which leads to a lower quality of the semi-polar AlN layer $(10\bar{1}1)$ compared to the structure of the AlN(MOCVD) buffer layer.

The quality of the epitaxial process was assessed by testing the growth of a polar AlN(0001) layer on a Si(111) substrate in one process. The value of ω_θ for the resulting AlN/Si(111) structure was ~ 1.0 arc. deg.

AFM study of the surface of the grown AlN layers showed that the block sizes of the semipolar lay-

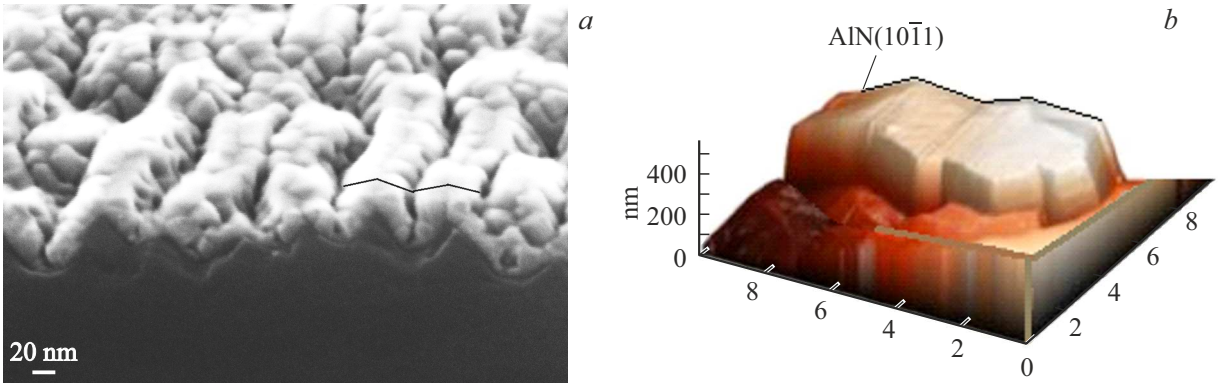

Figure 2. *a* — SEM image of the template AlN(MOCVD)/NP-Si(100); *b* — surface topography AlN/AlN(MOCVD)/NP-Si(100) structures with three coordinates (X, Y, Z).

ers during epitaxy on the template are significantly larger than on the substrate (Figure 1). AFM images of the surface of AlN/AlN(MOCVD)/NP-Si(100) and AlN(MOCVD)/NP-Si(100) stuctures show the „corrugated" surface character associated at the beginning with the nucleation and growth of blocks on surfaces tilted at 54° to the Si(100) plane of the nanogrooves (Figure 2, *a*), as noted in Ref. [16].

The surface profiles of the structures in the direction perpendicular to the grooves showed that the block size is $\sim 5\,\mu$m for the AlN/AlN(MOCVD)/NP-Si(100) structure (Figure 1, *a* and *b*) and $\sim 10\,\mu$m for the structure AlN/NP-Si(100) (Figure 1, *c* and *d*), and in the direction parallel to the groove, this difference is significantly greater (figures are not shown). It can be seen that the shape of the blocks is different: basically triangular pyramids for AlN/NP-Si(100) and mostly rectangular plates for AlN/AlN(MOCVD)/NP-Si(100) (Figure 1). However, we would like to note that at the initial stage of layer nucleation, the distance between the „ridges" of „corrugated" layer in the direction perpendicular to the grooves was ~ 70 nm, and this distance increased to $7\,\mu$m after HVPE epitaxy of $\sim 5\,\mu$m thick AlN layer (Figure 2).

The data obtained from studies of AlN layers grown on a substrate and template using X-ray diffraction analysis and AFM methods can be explained by differences in the nucleation rates of AlN layers in the MOCVD and HVPE methods and the diffusion lengths of Al atoms on the surfaces of the substrate and template of different composition and morphology.

By analogy with the model of growth of GaN [17], Al atoms in the gas phase are adsorbed on the surface of the substrate, and then diffuse to the surface of AlN crystals and can easily react with nitrogen atoms from the gas phase [18], contributing to the nucleation and growth of AlN crystals on Si(111) faces, which leads to the formation of semipolar-oriented blocks with AlN(10$\bar{1}$1) surface (Figure 2, *a*).

It is known that the effective diffusion length of Ga adatoms depends on the atmosphere in the reactor and can reach several micrometers at a temperature of 1040°C, depending on the flows of H_2, N_2 and NH_3 and the pressure during MOCVD epitaxy [19]. The change of the hydrogen atmosphere to argon in the case of GaN HVPE leads to a predominant growth of the layer in the direction tangential to the surface [18].

No diffusion length data in the argon atmosphere in the case of AlN HVPE are presented in the literature, but we assume that the diffusion length of the Al atom in the argon atmosphere in case of HVPE is significantly greater than in the hydrogen atmosphere in case of MOCVD. The migration of Al adatoms over the surface depends on the size of their diffusion barrier [20]. Al–N bond energy is 2.88 eV, and Al–Si bond energy is 3.43 eV [21]. It is known that the diffusion barrier on the Al(0001) surface is 1.17 eV for Al adatom, and the diffusion barrier on Si(111) surface is 1.25 eV [22]. In case of AlN HVPE grown on the template, Al atoms have a lower diffusion barrier and a longer time to embed in favorable lattice sites, which facilitates the fusion of grains into blocks with lower roughness. In addition, the data obtained on the size of blocks on the surface of AlN(10$\bar{1}$1) layers in case of HVPE in an argon atmosphere indicate a longer free path of Al adatom in the direction along the „ridges" than in the perpendicular direction.

Thus, the study results showed that growing AlN layers with a thickness of less than the height of the „ridges" of the structured surface, first by the MOCVD method, followed by cooling from the growth temperature to room temperature and subsequent growth by the HVPE method, results in smoother epitaxial layers that are promising for the purposes of gallium nitride electronics.

Funding

L.A. Sokura and Sh.Sh. Sharofidinov thank the Russian Science Foundation for the financial support of their research (project No. 24-22-00392).

Conflict of interest

The authors declare that they have no conflict of interest.

References

[1] R. Rounds, B. Sarkar, A. Klump, C. Hartmann, T. Nagashima, R. Kirste. Appl. Phys. Express, *11* (7), 071001 (2018). DOI: 10.7567/APEX.11.071001

[2] H. Yamashita, K. Fukui, S. Misawa, S. Yoshida. J. Appl. Phys., **50**, 896 (1979). DOI: 10.1063/1.326007

[3] D. Khachariya, S. Mita, P. Reddy, S. Dangi, J.H. Dycus, P. Bagheri, M.H. Breckenridge, R. Sengupta, Sh. Rathkanthiwar, R. Kirste, E. Kohn, Z. Sitar, R. Collazo, S. Pavlidis. Appl. Phys. Lett., **120**, 172106 (2022). DOI: 10.1063/5.0083966

[4] A. Krost, A. Dadgar. Mater. Sci. Eng. B, **93** (1–3), 77 (2002). DOI: 10.1016/S0921-5107(02)00043-0

[5] Y. Zhang, H. Long, J. Zhang, B. Tan, Q. Chen, S. Zhang, M. Shan, Z. Zheng, J. Dai, C. Chen. CrystEngComm, **21**, 4072 (2019). DOI: 10.1039/C9CE00589G

[6] L. Huang, Y. Li, W. Wang, X. Li, Y. Zheng, H. Wang, Z. Zhang, G. Li. Appl. Surf. Sci., **435**, 163 (2018). DOI: 10.1016/j.apsusc.2017.11.002

[7] H. Masui, S. Nakamura, S.P. DenBaars, U.K. Mishra. IEEE Trans. Electron. Dev., **57**, 88 (2010). DOI: 10.1109/TED.2009.2033773

[8] T. Takeuchi, H. Amano, I. Akasaki. Jpn. J. Appl. Phys., **39**, 413 (2000). DOI: 10.1143/JJAP.39.413

[9] A.E. Romanov, T.J. Baker, S. Nakamura, J.S. Speck. J. Appl. Phys., **100**, 023522 (2006). DOI: 10.1063/1.2218385

[10] A.M. Smirnov, E.C. Young, V.E. Bougrov, J.S. Speck, A.E. Romanov. J. Appl. Phys., **126**, 245104 (2019). DOI: 10.1063/1.5126195

[11] V.N. Bessolov, E.V. Konenkova, V.N. Panteleev. ZhTF, **90** (12), 2123 (2020). (in Russian). DOI: 10.21883/JTF.2020.12.50130.98-20

[12] Z.-Z. Zhang, J. Yang, D.-G. Zhao, F. Liang, P. Chen, Z.-S. Liu. Chin. Phys. B, **32**, 028101 (2023). DOI: 10.1088/1674-1056/ac6b2b

[13] A. Bardhan, S. Raghavan. J. Cryst. Growth, **578**, 126418 (2022). DOI: 10.1016/j.jcrysgro.2021.126418

[14] B.T. Tran, H. Hirayama, N. Maeda, M. Jo, S. Toyoda, N. Kamata. Sci. Rep., **5**, 14734 (2015). DOI: 10.1038/srep14734

[15] J. Shen, X. Yang, D. Liu, Z. Cai, L. Wei, N. Xie, F. Xu, N. Tang, X. Wang, W. Ge, B. Shen. Appl. Phys. Lett., **117**, 022103 (2020). DOI: 10.1063/5.0010285

[16] V.N. Bessolov, E.V. Konenkova. ZhTF, **93** (9), 1235 (2023). (in Russian). DOI: 10.21883/JTF.2023.09.56211.31-23

[17] S. Naritsuka, T. Kondo, H. Otsubo, K. Saitoh, Y. Yamamoto, T. Maruyama. J. Cryst. Growth, **300** (1), 118 (2007). DOI: 10.1016/j.jcrysgro.2006.11.002

[18] V.N. Bessolov, V.M. Botnariuk, Yu.V. Zhilyaev, E.V. Konenkova, N.K. Poletaev, S.D. Rayevsky, S.N. Rodin, S.L. Smirnov, Sh.Sharofidinov, M.P. Shcheglov, H.S. Park, M. Koike. Pis'ma ZhTF, **32** (15), 60 (2006). (in Russian).

[19] M.M. Rozhavskaya, W.V. Lundin, S.I. Troshkov, A.F. Tsatsulnikov, V.G. Dubrovskii. Phys. Status Solidi A, **212** (4), 1 (2015). DOI: 10.1002/pssa.201431912

[20] C. Tholander, B. Alling, F. Tasnadi, J.E. Greene, L. Hultman. Surf. Sci., **630**, 28 (2014). DOI: 10.1016/j.susc.2014.06.010

[21] D. Tzeli, I.D. Petsalakis, G. Theodorakopoulos. J. Phys. Chem. C, **113**, 13924 (2009).

[22] V. Jindal, F. Shahedipour-Sandvik. J. Appl. Phys., **105**, 084902 (2009). DOI: 10.1063/1.3106164

Translated by A.Akhtyamov